

EFFECT OF CYCLIC STRAIN RATE AND SULFIDES ON ENVIRONMENTALLY ASSISTED CRACKING BEHAVIORS OF SA508 GR. 1A LOW ALLOY STEEL IN DEOXYGENATED WATER AT 310°C

HUN JANG¹, HYUNCHUL CHO¹, CHANGHEUI JANG^{1*}, TAE SOON KIM² and CHAN KOOK MOON²

¹Department of Nuclear and Quantum Engineering Korea Advanced Institute of Science and Technology
373-1 Guseong-dong, Yuseong-gu, Daejeon 305-701, Republic of Korea

²Nuclear Engineering and Technology Institute Korea Hydro and Nuclear Power Co., Ltd.,
25-1, Jang-dong, Yuseong-gu, Daejeon 305-343, Republic of Korea

*Corresponding author. E-mail : chjang@kaist.ac.kr

Received July 2, 2007

Accepted for Publication January 21, 2008

To understand the effect of the cyclic strain rate on the environmentally assisted cracking behaviors of SA508 Gr.1a low alloy steel in deoxygenated water at 310°C, the fatigue surface and a sectioned area of specimens were observed after low cycle fatigue tests. On the fatigue surface of the specimen tested at a strain rate of 0.008 %/s, unclear ductile striations and a blunt crack tip were observed. Therefore, metal dissolution could be the main cracking mechanism of the material at this strain rate. On the other hand, on the fatigue surfaces of the specimens tested at strain rates of 0.04 and 0.4 %/s, brittle cracks and flat facets, which are evidences of the hydrogen induced cracking, were observed. In addition, a tendency of linkage between the main crack and the micro-cracks was observed on the sectioned area. Therefore, at higher strain rates, the main cracking mechanism could be hydrogen induced cracking. Additionally, evidence of the dissolved MnS inclusions was observed on the fatigue surface from energy dispersive x-ray spectrometer analyses. Thus, despite the low sulfur content of the test material, the sulfides seem to contribute to environmentally assisted cracking of SA508 Gr.1a low alloy steel in deoxygenated water at 310°C.

KEYWORDS : Environmentally Assisted Cracking, Low Cycle Fatigue, Low Alloy Steel, Hydrogen Induced Cracking, MnS Inclusion, Metal Dissolution

1. INTRODUCTION

Low alloy steels (LASs) used as the structural materials of nuclear power plants (NPPs) are subject to cyclic stress during plant operation. Consequently, fatigue damage is one of the most significant degradation mechanisms of them. Moreover, fatigue crack growth rate is accelerated in the high temperature water environment of NPPs, thereby reducing the fatigue life [1-6]. Therefore, the environmental fatigue behaviors of LASs should be considered to assess the integrity and the safety of NPPs. To date, many studies have been done to evaluate the environmental fatigue behaviors of LASs [1-9]. It has been reported that the reduction of fatigue life is related to environmentally assisted cracking (EAC) mechanisms, such as metal dissolution and hydrogen induced cracking (HIC) [1-6].

In the metal dissolution mechanism, the protective oxide film is ruptured under tensile strain, and the metal is dissolved

by exposure to a corrosive environment until a protective oxide layer is formed [1-4]. The whole process is repeated, resulting in crack growth. In the HIC mechanism, hydrogen atoms produced by corrosion reaction are absorbed by the metal and concentrated at strong hydrogen trapping sites, which increases stress in a localized area [1-6,10]. Then, crack growth occurs by the brittle cracking caused by the high stress [1-6].

Meanwhile, it is well known that environmental effects on the fatigue life decrease with decreasing sulfur content [7,11-14]. As sulfides can prevent the recombination of hydrogen at the crack tip and sulfate anions are aggressive in terms of increasing the oxidation rate, the dissolution of MnS inclusions is known to accelerate the crack growth by both EAC mechanisms [5,11-15]. However, the values of S contents below which environmental effects are negligible or above which the effects of sulfide on EAC may saturate were not well defined due to the lack of available data [7]. Especially, in low dissolved-oxygen

water, the effects of sulfur on EAC mechanisms could be influenced by various factors and is not clearly understood.

In this study, the effect of cyclic strain rate on environmental fatigue resistance was investigated to understand the EAC behaviors of SA508 Gr. 1a LAS in deoxygenated water at 310°C. In addition, energy dispersive x-ray spectrometer analyses (EDS) were performed on fatigue surfaces to investigate the effects of sulfides on environmental fatigue behaviors.

2. EXPERIMENTAL DETAILS

2.1 Material and Tensile Test

The test material was an ASME SA508 Gr. 1a LAS used as the material for reactor coolant system piping.

The material was normalized at 920°C for 10 minutes, followed by quenching in water, and then tempered at 650°C for 130 minutes in air. The chemical compositions were analyzed, and the results are summarized in Table 1. The tensile properties were measured using round bar specimens with a 4 mm gauge diameter in air at room temperature (RT) and 310°C. The average values of 3 test results are shown in Table 2.

2.2 Low Cycle Fatigue Test System and Test Conditions

The test specimen was a smooth round bar type with a 19.05 mm gauge length and a 9.63 mm gauge diameter [4]. The low cycle fatigue (LCF) test system is shown in Fig. 1. Test conditions of the LCF test are given in Table 3. The fatigue life, N_{25} , was defined as the number of

Table 1. The Chemical Composition of SA508 Gr. 1a LAS (wt. %)

| | | | | | | | | | |
|------|------|------|-------|-------|------|------|------|------|------|
| C | Si | Mn | P | S | Ni | Cr | Mo | Cu | Al |
| 0.22 | 0.21 | 1.16 | 0.008 | 0.004 | 0.20 | 0.17 | 0.04 | 0.12 | 0.02 |

Table 2. Tensile Properties of SA508 Gr. 1a LAS

| Y.S. (MPa) | | U.T.S. (MPa) | | Elong. (%) | |
|------------|-------|--------------|-------|------------|-------|
| RT | 310°C | RT | 310°C | RT | 310°C |
| 350.8 | 243.3 | 521.2 | 521.9 | 39.2 | 38.3 |

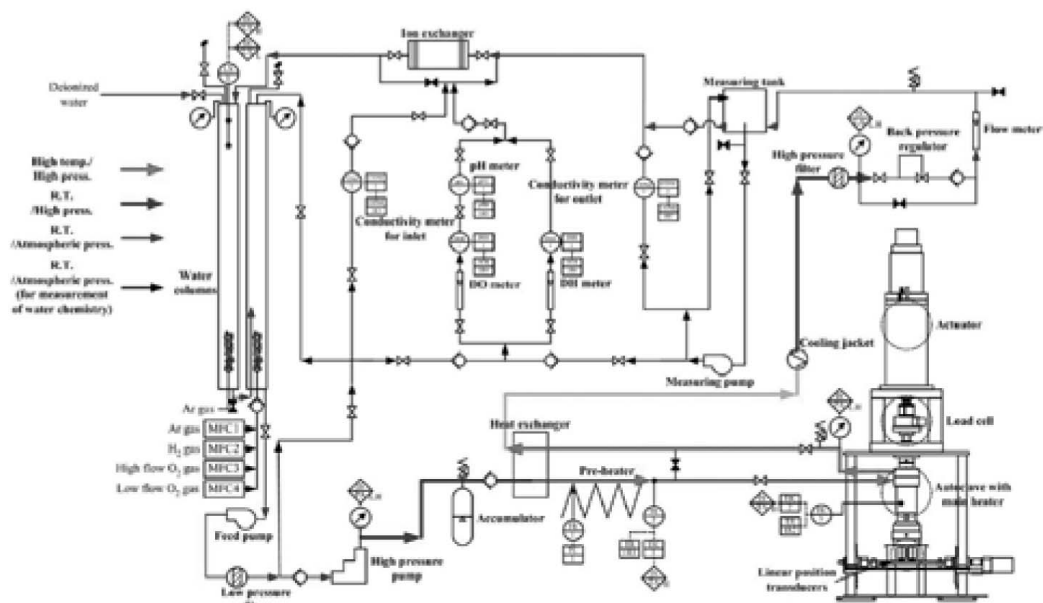


Fig. 1. Low Cycle Fatigue Test System

cycles at which the tensile stress drops 25 % from its peak value. After the LCF test was finished, the fatigue surface and the sectioned area of the specimen tested at 0.4% strain amplitude were observed using scanning electron microscope (SEM), and EDS analysis was performed to find MnS inclusions on the fatigue surface of the tested materials. Before the SEM observation, the oxides on the fatigue surface were removed with a solution containing 7 g of 2-Butyne 1.4 diol, 16 cc of HCl, and 220 cc of distilled water.

Table 3. Test Conditions of Low Cycle Fatigue Test of SA508 Gr. 1a LAS

| | |
|------------------|---|
| Wave form | Fully reversed triangular |
| Strain rate | 0.008, 0.04, 0.4 %/s |
| Strain amplitude | 0.4, 0.6, 0.8, 1.0 % |
| Test environment | Air at RT and 310 °C, Deoxygenated water at 310 °C |
| Dissolved oxygen | < 1 ppb |
| Conductivity | < 0.1 μ S/cm |

3. RESULTS

3.1 Fatigue Life of SA508 Gr. 1a LAS

Figure 2 shows the fatigue life test results for SA508 Gr.1a LAS at various loading conditions in various environments. For comparison, ASME design and mean curves are also shown in the figure. Also shown in the figure is the minimum curve for the data scatter of factor 2 including material variability. As shown in the figure,

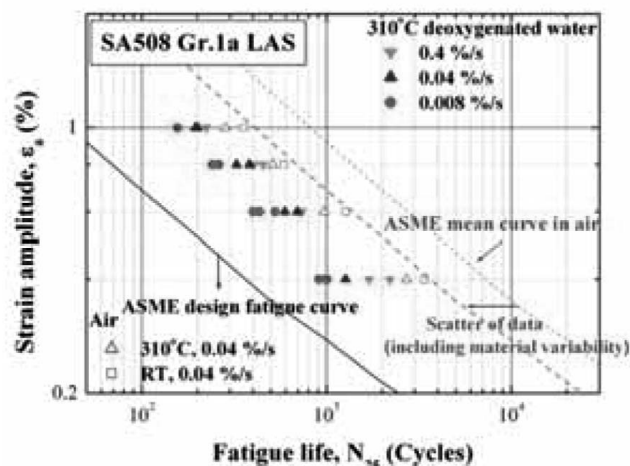


Fig. 2. The Fatigue Life of SA508 Gr. 1a LAS [1]

the fatigue life in deoxygenated water at 310°C was shorter than that in air. Moreover, the fatigue life in deoxygenated water at 310°C was reduced with a decreasing strain rate, from 0.4 to 0.008 %/s.

3.2 Fatigue Surface Observation

Figure 3 shows the fatigue surfaces of the specimens tested in air at RT and in deoxygenated water at 310°C. The fatigue crack features on the surfaces depended on the test environment and the loading conditions. As shown in Fig. 3 (a), well-developed ductile striations were observed on the fatigue surface of the specimen tested in air at RT. However, unclear ductile striations were observed on the fatigue surface of the specimen tested in deoxygenated water at 310°C at a strain rate of 0.008 %/s, as shown in Fig. 3 (b). In addition, as shown in Figs. 3 (c) and (d), brittle cracks and flat facets were generally observed on the fatigue surfaces of the specimen tested at strain rates of 0.04 and 0.4 %/s. Pore-like features were also observed on the fatigue surface of the specimen tested at all strain rates in deoxygenated water at 310°C.

3.3 Sectioned Area Observation

Figure 4 shows the sectioned areas of the specimens tested in various test conditions. As shown in Fig. 4 (a), a sharp and clear crack tip was observed on the sectioned area of the specimen tested in air at RT. However, in the case of the sectioned areas of the specimens tested in deoxygenated water at 310°C, blunt crack tips were observed, as shown in Figs. 4 (b), (c), and (d). In addition, the characteristics of the fatigue crack of the specimens tested in deoxygenated water at 310°C changed with various strain rates. As shown in Fig. 4 (c), micro-cracks were observed around the blunt main crack in the specimen tested at a strain rate of 0.04 %/s. As shown in the figure, some micro-cracks were about to link with the main crack. In addition, as shown in Fig. 4 (d), a tendency of crack linkage was observed for the specimen tested at a strain rate of 0.4 %/s.

3.4 EDS Analysis

Figure 5 shows a pore-like site with a brittle crack on the fatigue surface of the specimen tested at a strain rate of 0.008%/s in deoxygenated water at 310°C. The average values of sulfur and manganese contents on the fatigue surface and on pore surface are also shown in Fig. 5. While sulfur was not detected on the fatigue surface, sulfur and manganese contents were higher on the pore surfaces. This could indicate that the pore-like sites are the residue of the MnS inclusions.

4. DISCUSSION

4.1 EAC Mechanisms

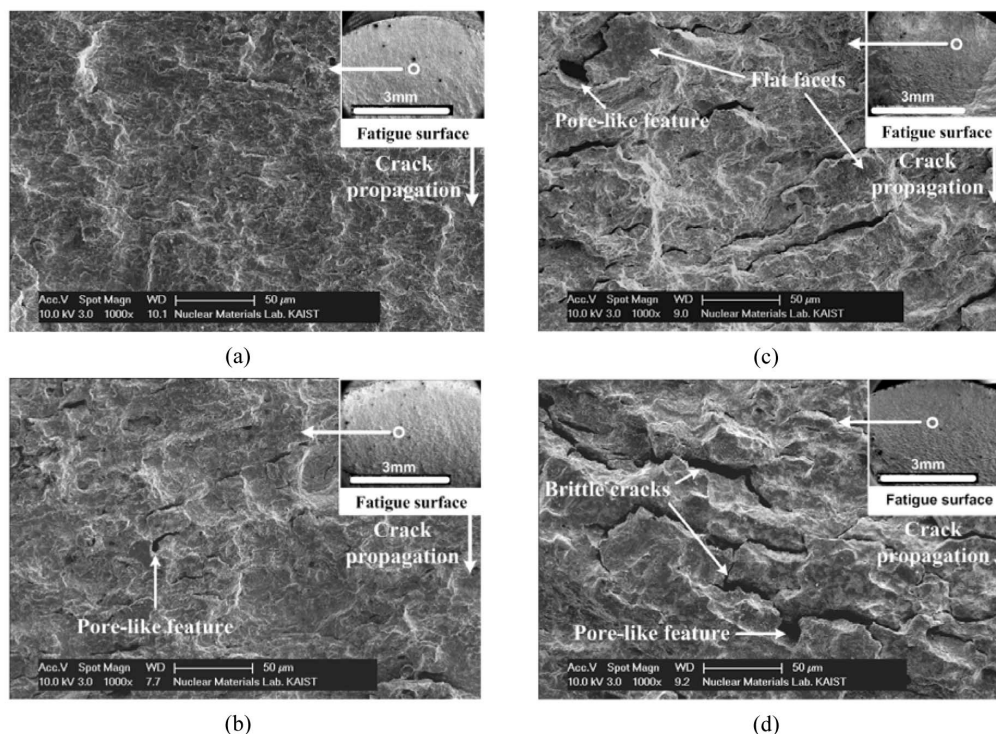


Fig. 3. Fatigue Surfaces of the Specimens Tested at a Strain Amplitude of 0.4 % and Strain Rates of (a) 0.04 %/s in Air at RT, (b) 0.008, (c) 0.04, and (d) 0.4 %/s in Deoxygenated Water at 310°C

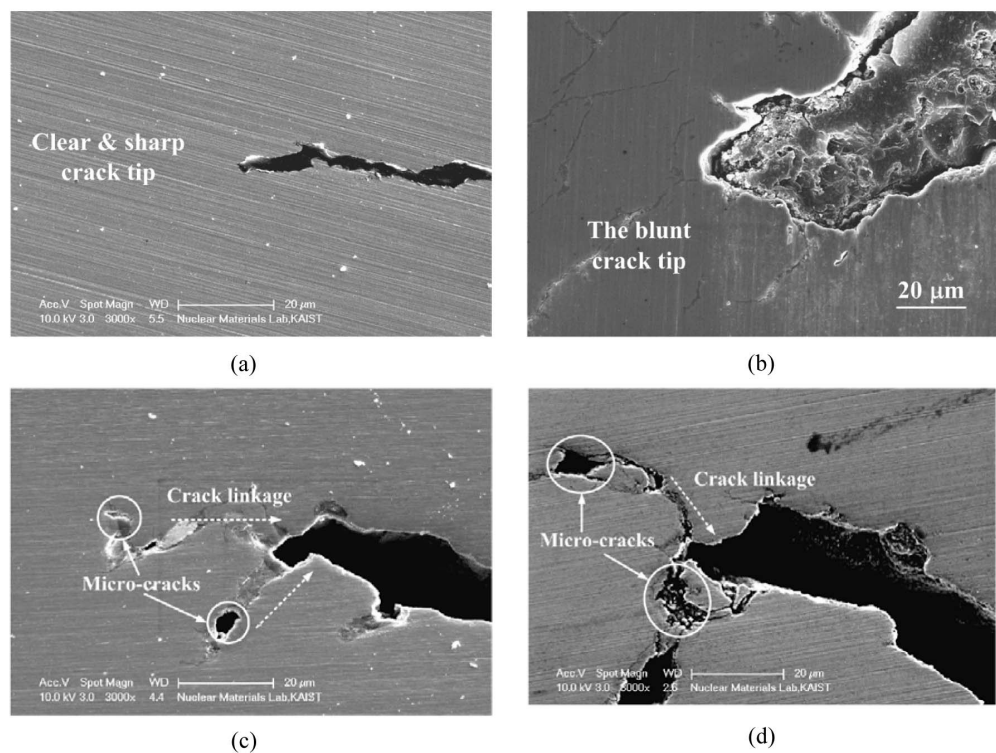
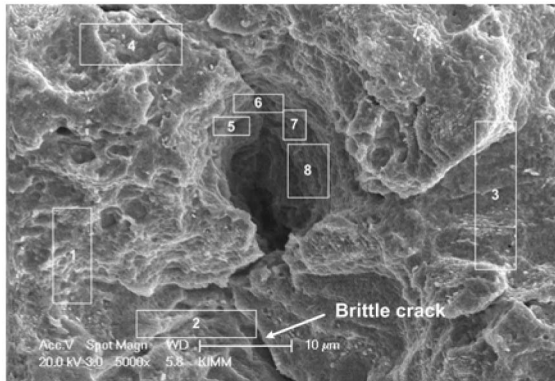


Fig. 4. Sectioned Areas of the Specimens Tested at a Strain Amplitude of 0.4 % and Strain Rates of (a) 0.04 %/s in Air at RT, (b) 0.008, (c) 0.04, and (d) 0.4 %/s in Deoxygenated Water at 310°C



Semiquantitative EDX analysis (avg. wt. %)

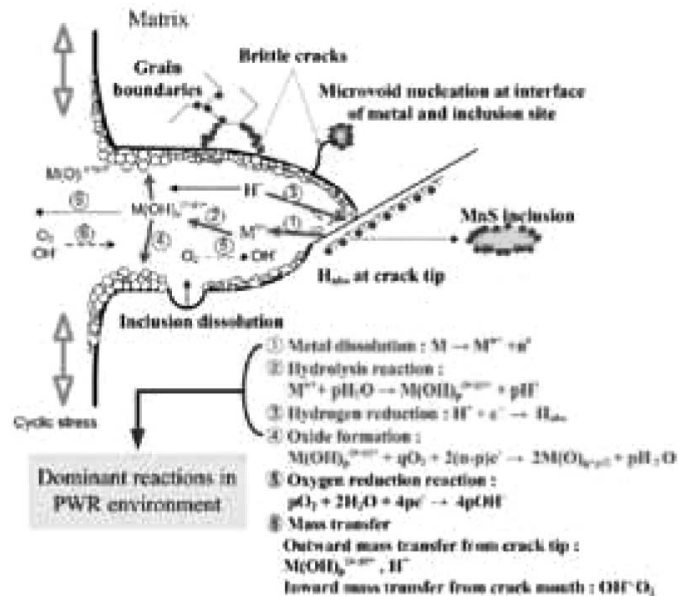
| Location | Fe | S | Mn |
|----------------------------------|-------------|-------------|-------------|
| Fatigue surface (1 – 4) | 98.7 | 0.00 | 1.30 |
| Pore surface (5 – 8) | 95.0 | 1.01 | 3.93 |

Fig. 5. The Dissolved Inclusion Around the Brittle Crack in the Fatigue Surface of Specimen Tested at a Strain Rate of 0.008 %/s in Deoxygenated Water at 310°C

From the results of the LCF test of SA508 Gr. 1a LAS [1], the fatigue life in deoxygenated water at 310°C was shorter than that in air. As mentioned above, it is well known that the reduction of fatigue life is related to EAC mechanisms. The probable EAC mechanisms involved are metal dissolution and HIC [1-7]. Figure 6 shows a schematic illustration of EAC mechanisms. The process of the metal dissolution mechanism can be described as follows: (i) formation of a protective oxide film at the crack tip, (ii) rupture of the oxide film by applied strain, (iii) exposure of fresh bare metal to the corrosive environment, (iv) the dissolution of the freshly exposed metal, and (v) repetition of steps (i) – (iv), which results in the increase of crack growth rate [1-5,11].

On the other hand, the process of the HIC can be described as follows. First, the hydrogen atoms are absorbed at the crack tip during the crack opening period. Absorbed hydrogen is transported to the local stressed region along a stress gradient, such as the grain boundaries and the interface of inclusion/matrix and dislocations, which are strong trapping sites for the absorbed hydrogen [1-6,10]. Consequently, hydrogen atoms can accumulate in those regions and thereby increase the local stress [1-6,16]. In this way, hydrogen can contribute to the reduction of fatigue life in high temperature water.

Schematic illustration of EAC mechanisms



Cyclic strain rate dependence of EAC mechanisms

At lower strain rate \rightarrow Crack tip strain rate $\downarrow \rightarrow$ Rupture rate of oxide film $\downarrow \rightarrow$ Exposure of fresh bare metal $\downarrow \rightarrow$ Hydrogen absorption $\downarrow \rightarrow$ HIC \downarrow relatively

At higher strain rate \rightarrow Crack tip strain rate $\uparrow \rightarrow$ Rupture rate of oxide film $\uparrow \rightarrow$ Exposure of fresh bare metal $\uparrow \rightarrow$ Hydrogen absorption $\uparrow \rightarrow$ HIC \uparrow relatively

Fig. 6. Schematic Illustration of EAC Mechanisms

From the SEM images shown in Fig. 3 and Fig. 4, the features relevant to the EAC mechanisms were evident on the fatigue surface and the sectioned area. From the microstructure observation of the specimen tested in deoxygenated water at 310°C, evidence of the metal dissolution mechanism, such as unclear ductile striations and a blunt crack tip, was observed. In addition, evidence of the HIC mechanism, such as brittle cracks, flat facets, and micro-cracks, was also observed. The brittle cracks and the flat facets could be generated by an increase in local stress at high hydrogen concentration regions, such as grain boundaries and the interface of inclusions and metal [16]. Therefore, both EAC mechanisms are responsible for the reduction of fatigue life in high temperature water. Furthermore, since the EAC mechanisms are influenced by a loading factor, such as cyclic strain rate [1-6], the fatigue crack features depended on the applied strain rate during the LCF test.

4.2 Strain Rate Dependence of EAC Mechanism

As mentioned above, the fatigue crack features of the specimens tested in deoxygenated water at 310°C changed with the applied strain rate. As shown in Figs. 3 (b) and 4 (b), the unclear ductile striations and the blunt crack tip were dominantly observed for the specimen tested at a strain rate of 0.008 %/s. From these unclear striations and blunt crack shape, the metal dissolution could be considered as the dominant EAC mechanism at a strain rate of 0.008 %/s [1-2]. On the other hand, as shown in Figs. 3 (c) and (d), many brittle cracks and flat facets were observed on the fatigue surfaces. Micro-cracks with blunt crack tip were observed on the sectioned areas shown in Figs. 4 (c) and (d). These fatigue crack features could indicate that the HIC plays the most important role in the acceleration of the fatigue crack growth rate at strain rates of 0.04 and 0.4 %/s [1-2].

Figure 6 illustrates cyclic strain rate dependence on EAC mechanisms. During cyclic loading, the slower cyclic strain rate may provide relatively longer crack opening time. The increase in crack opening time brings out not only the sufficient time for hydrogen absorption but also diffusion of O_2 from bulk solution [5]. The diffusion of O_2 is believed to promote the protective oxide formation reaction at the crack tip, and the oxide layer may act as a strong barrier to absorption of hydrogen [1-6]. Therefore, although the hydrogen absorption time increases sufficiently, HIC could be retarded [2]. In addition, as the rupture rate of oxide film is proportional to the applied strain rate, the low rupture rate of oxide film may occur at the crack tip at a lower strain rate, thereby lowering the exposure time of fresh bare metal [1-4]. This situation would decrease the absorption of hydrogen into the matrix. Therefore, at lower strain rates, the dominant EAC mechanism of LAS may be metal dissolution [1-2]. On the other hand, at higher strain rate, the crack opening time could decrease, thereby decreasing the hydrogen absorption time. However,

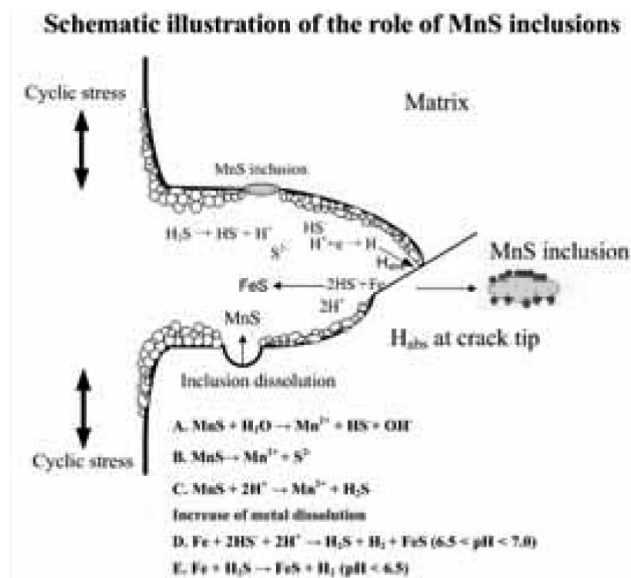


Fig. 7. Schematic Illustration of the Role of MnS Inclusions

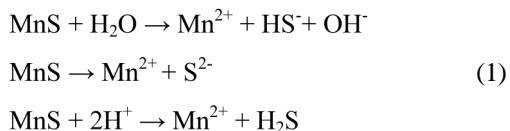
the fresh bare metal may be easily exposed to a corrosive environment due to the higher rupture rate of oxide film. This may lead to the absorption of hydrogen into the matrix. Therefore, the HIC mechanism may be the main EAC mechanism at relatively faster strain rates [1-2].

Therefore, from the observation of the fatigue surfaces and the sectioned areas of the specimens tested at various strain rates in deoxygenated water at 310°C, it is thought that metal dissolution is the dominant EAC mechanism at a strain rate of 0.008 %/s and that HIC affects significantly the fatigue crack propagation at strain rates of 0.04 and 0.4 %/s.

4.3 The Role of MnS in the EAC Mechanism

Although the sulfur content of LAS used in this study was very low, evidence of dissolved inclusion was easily observed on the fatigue surface tested in deoxygenated water at 310°C, as shown in Fig. 5. From the EDS analysis, it is thought that MnS inclusions were dissolved in corrosive environment, because the sulfur and manganese contents in the dissolved inclusion site were higher than those in other areas on the fatigue surface. The brittle crack around the MnS inclusion may be generated by an increase in local stress at the interface of MnS inclusion and matrix, because the absorbed hydrogen could be easily diffused in that region [10,16-17]. Therefore, MnS inclusion sites could have contributed to the HIC mechanism.

Furthermore, it is well known that the dissolved sulfides could contribute to the acceleration of the EAC mechanism [11-14]. Figure 7 illustrates the role of sulfides in the crack tip. As shown in Fig. 7, the sulfides are readily dissolved in the elevated temperature water [12]. The dissolved MnS may be decomposed by the following reactions [5].



The sulfides produced by reactions in (1) could interact with Fe, thereby increasing metal dissolution [12]. Therefore, the sulfides anions are aggressive in terms of increasing the oxidation rate [11-12]. Also, the sulfides, S^{2-} , HS^- , H_2S produced by above reactions may act as poison to prevent the recombination of hydrogen and promote the absorption of hydrogen into metal, thereby increasing HIC [5,12,15].

To enhance the EAC mechanism, a critical concentration of the sulfides is required at the crack tip environment [7,13]. Since the increase of the sulfur content in metal could increase the concentration of sulfides at the crack tip, the low sulfur steel including SA508 Gr. 1a LAS is less susceptible to EAC than high sulfur steels [7,12-13]. Additionally, it has been reported that low sulfur steels (< 0.005 wt.-% S) should be considered when environment is aerated water (1ppm DO) [7]. Therefore, the effect of sulfides in the low sulfur steels could be an important factor in a boiling water reactor (BWR) environment.

However, Chopra [7] reported that the available data sets are too sparse to establish a functional form for dependence of fatigue life on sulfur content or to define a threshold for sulfur content. Also, Atkinson [12] reported that the corrosion fatigue crack growth rate and threshold stress intensity factor were functions of the S content in the range of 0.003 – 0.019 wt.-% in a pressurized water reactor (PWR) condition, while a clear relationship between the fatigue propagation rate and the steel sulfur content has not been observed [12]. Therefore, the dissolved sulfides may contribute to enhance the EAC mechanism in SA508 Gr. 1a LAS containing sulfur content of 0.004 wt.-%. Moreover, it is likely that the effect of the dissolved sulfide on the EAC mechanism could be sufficiently increased by the synergistic effect of various factors [12,18]. However, as the present work does not provide sufficient evidence to evaluate the effect of sulfide on the EAC mechanism, it is not fully understood how much the sulfides contribute to the enhancement of EAC. Therefore, additional tests on high sulfur containing LAS are required to evaluate the effect of sulfides on EAC behaviors of SA508 Gr. 1a LAS in high temperature water.

5. CONCLUSIONS

1. The fatigue life of SA508 Gr. 1a LAS in deoxygenated water at 310°C was shorter than that in air and depended on strain rates. It is thought that the reduction in the fatigue life is accelerated by EAC mechanisms.
2. From microstructure observation, evidence of metal

dissolution, such as unclear ductile striations and the blunt crack tip, were observed mainly at a strain rate of 0.008 %/s. On the other hand, evidence of HIC, such as brittle cracks, flat facets, and micro-cracks, was observed at strain rates of 0.04 and 0.4 %/s. In addition, fatigue crack propagation with linkage between a blunt main crack and micro-cracks was observed mainly at a strain rate of 0.04 %/s.

3. From EDS analysis, high sulfur content was detected on the surfaces of the holes which were the former MnS inclusion site. In addition, brittle cracks around the holes were observed. These could be the evidence of HIC induced by the hydrogen absorbed in the interface of inclusion and matrix, and the dissolved MnS inclusion could contribute to acceleration of EAC mechanism. Therefore, despite the low sulfur content of the test material, the sulfides seem to contribute to environmentally assisted cracking of SA508 Gr.1a low alloy steel in deoxygenated water at 310°C.

ACKNOWLEDGEMENTS

This study was mainly supported by the Korea Hydro and Nuclear Power Co., Ltd. and partly by the Second Phase BK21 Program of the Ministry of Education, Science and Technology of Korea.

REFERENCES

- [1] H. Cho, H. Jang, B.K. Kim, C. Jang, and I.S. Kim, "Environmental Fatigue Behaviors of SA508 Gr.1a Low Alloy Steel in 310°C Deoxygenated Water," *Key Eng. Mater.*, **345-346**, 1039 (2007).
- [2] H. Cho, H. Jang, B.K. Kim, I.S. Kim, and C. Jang, "Effect of Cyclic Strain Rate on Environmental Fatigue Behaviors of SA508 Gr.1a Low Alloy Steel in 310°C Deoxygenated Water," *Adv. Mater. Res.*, **26-28**, 1121 (2007).
- [3] H. Cho, B.K. Kim, I.S. Kim and C. Jang, "Low Cycle Fatigue Behaviors of Type 316LN Austenitic Stainless Steel in 310°C Deaerated Water - Fatigue Life and Dislocation Structure Development," *Mat. Sci. Eng. A*, **476**, 248 (2008).
- [4] H. Cho, B.K. Kim, I.S. Kim, C. Jang, and D.Y. Jung, "Fatigue Life and Crack Growth Mechanisms of the Type 316LN Austenitic Stainless Steel in 310°C Deoxygenated Water," *J. Nucl. Sci. Technol.*, **44**, 1007 (2007).
- [5] X.Q. Wu and Y. Katada, "Strain Rate Dependence of Low Cycle Fatigue Behavior in A Simulated BWR Environment," *Corros. Sci.*, **47**, 1415 (2005).
- [6] X.Q. Wu, E. Han, W. Ke, and Y. Katada, "Effect of Loading Factor on Environmental Fatigue Behavior of Low Alloy Pressure Vessel Steels in Simulated BWR Water," *Nucl. Eng. Des.*, **237**, 1452 (2007).
- [7] O.K. Chopra and W.J. Shack, "Effect of LWR Coolant Environments on the Fatigue Life of Reactor Materials," NUREG/CR-6909, Argonne National Laboratory (2006).
- [8] H.S. Mehta and S.R. Gosselin, "Environmental Factor Approach to Account of Water Effects in Pressure Vessel and Piping Fatigue Evaluation," *Nucl. Eng. Des.*, **181**, 175 (1998).
- [9] F.A. Simonen, M.A. Khaleel, H.K. Phan, D.O. Harris, D.D.

- Dedhia, D.N. Kalinousky, and S.K. Shaukat, "Evaluation of Environmental Effects on Fatigue Life of Piping," *Nucl. Eng. Des.*, **208**, 143 (2001).
- [10] T. Otsuka and T. Tanabe, "Hydrogen Diffusion and Trapping Process around MnS Precipitates in Fe Examined by Tritium Autoradiography," *J. Alloy Compd.*, **425** (2007).
- [11] F.P. Ford and P.W. Emigh, "The Prediction of the Maximum Corrosion Fatigue Crack Propagation Rate in the Low Alloy Steel Deoxygenated Water System at 288°C," *Corros. Sci.*, **25**, 673 (1985).
- [12] J.D. Atkinson, J. Yu and Z-Y. Chen, "An Analysis of the Effects of Sulphur Content and Potential on Corrosion Fatigue Crack Growth in Reactor Pressure Vessel Steels," *Corros. Sci.*, **38**, 755 (1996).
- [13] L.A. James, "Technical Basis for the Initiation and Cessation of Environmentally Assisted Cracking of Low Alloy Steels in Elevated Temperature PWR Environments," Westinghouse Electric Company (1997).
- [14] J. D. Atkinson and J. E. Forrest, "Factors Influencing the Rate of Growth of Fatigue Cracks in RPV Steels Exposed to a Simulated PWR Primary Water Environment," *Corros. Sci.*, **25**, 607 (1985).
- [15] D.A. Jones, *Principles and Prevention of Corrosion*, **3rd ed.**, p. 457, Prentice Hall Inc. (1995).
- [16] S.P. Lynch, "Hydrogen Effects on Material Behavior and Corrosion Deformation Interactions," *Proc. Int. Conf. Hydrogen Effects on Material Behavior and Corrosion Deformation Interactions*, Jackson Lake Lodge, Moran, Wyoming, USA, Sep. 22-26, 2002.
- [17] S.G. Lee, C. Jang, and I.S. Kim, "Effects of Hydrogen on the Fatigue Crack Growth Rate of Low Alloy Steels," *Proc. Int. Congress on Advanced Nuclear Power Plant (ICAPP'06)*, Reno, NV, USA, June 4-8, 2006.
- [18] J.D. Atkinson, J. Yu, Z.Y. Chen and Z.J. Zhao, "Modelling of Corrosion Fatigue Crack Growth Plateau for RPV Steels in High Temperature Water," *Nucl. Eng. Des.*, **184**, 13 (1998).